Supporting Information

Surface-initiated passing-through polymerization on a rubber substrate: Supplying monomer from swollen substrates

Sean T. McDermott[‡], Shawn P. Ward[†], Ngoc Chau H. Vy[‡], Zilu Wang, [§] Mayra Daniela Morales-Acosta[†], Andrey V. Dobrynin, [§*] Douglas H. Adamson[†‡*]

[†] Polymer Program, Institute of Materials Science, University of Connecticut, Storrs CT 06269

[‡] Department of Chemistry, University of Connecticut, Storrs CT 06269

[§] Department of Chemistry, University of North Carolina, Chapel Hill NC 27599

Correspondence Author. Email: douglas.adamson@uconn.edu; avd@email.unc.edu
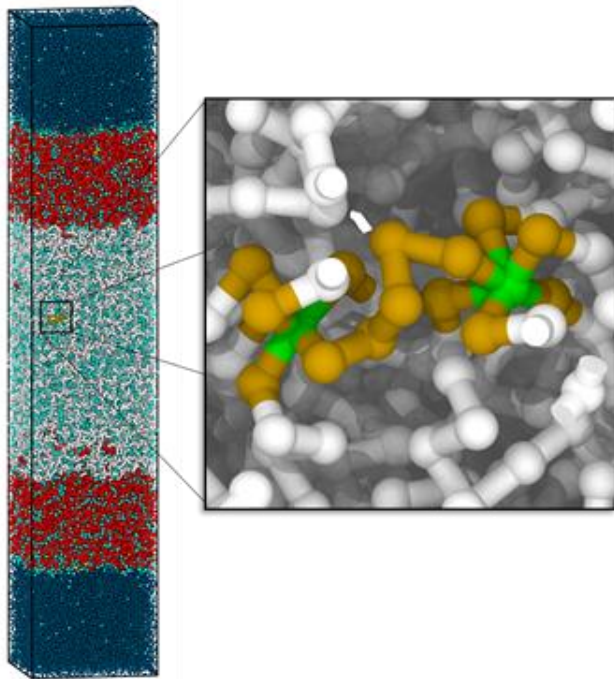
Simulation Details

Figure S1.1 Snapshot of the simulation box. Brush chains are shown by red beads, catalytic sites at the chain ends are colored in yellow, monomers and solvent beads are shown by light and dark blue beads respectively, beads belonging to network strands are shown in gray.

We performed molecular dynamics simulations[1] of the brush polymerization by "passing through" approach in which monomers were supplied from swollen network to chains growing from network surface. Our simulations used a coarse-grained representation of monomers, solvents, growing polymer chains, and brush supporting network (see **Figure S1.1**). We modeled growing polymer chains by bead-spring chains consisting of beads with diameter σ grafted to each junction point on the network surface. The network had cubic symmetry with $10 \times 10 \times 20$ and $10 \times 10 \times 10$ junction points connected by chains made of 5 beads (6 connecting bonds, representing a smaller mesh size network) and 11 beads (12 connecting bonds, a larger mesh size network) to their neighbors.

All beads in the system interacted through truncated-shifted Lennard Jones potential:

$$U_{LJ}(r) = \begin{cases} 4\varepsilon_{LJ}\big(f(\sigma/r) - f(\sigma/r_{cut})\big) & r < r_{cut} \\ 0 & r \geq r_{cut} \end{cases} \qquad (SI1.1)$$

where function,

$$f(x) = x^{12} - x^6 \qquad\qquad\qquad\text{(SI1.2)}$$

the Lennard-Jones interaction parameters for different bead pairs ε_{LJ} are listed in **Table S1.1** and the cut-off radius r_{cut}=2.5 σ. This selection of interaction parameters maintains similar densities in pure component phases and, at the same time, induces phase separation between dissimilar species with a narrow interface.

Table S1.1 Interaction parameters

ε_{LJ}	M	S	A	N	P
M	1.0	0.5	1.0	1.0	1.0
S	0.5	1.0	0.5	0.5	0.5
A	1.0	0.5	1.0	1.0	1.0
N	1.0	0.5	1.0	1.0	1.0
P	1.0	0.5	1.0	1.0	1.0

M - monomers, S - solvent, A - active monomers (catalytic sites), N - network beads, P - polymer beads.

The connectivity of beads into brush chains and polymer network was maintained by the FENE bonds with

$$U_{FENE}(r) = -\frac{1}{2}KR_0^2\ln\left(1 - \frac{r^2}{R_0^2}\right) \qquad\qquad\text{(SI1.3)}$$

where the spring constant K=30 $k_B T$ and the maximum bond length R_0=1.5 σ. The repulsive part of the bond potential is given by the pure repulsive WCA potential with ε_{LJ}=1.0 $k_B T$ and r_{cut}=$2^{1/6}$ σ (see eq SI1.1).

We carried out simulations in a constant number of particles, pressure, and temperature ensemble (NPT) with external pressure set to P=1.0 $k_B T/\sigma^3$ and 3-D periodic boundary conditions. The constant temperature and pressure were maintained by coupling the system to a Nosé-Hoover style thermostat (T_{damp}=1.0 τ_{LJ}^{-1}) and barostat in z and xy directions, respectively (P_{damp}=1.0τ_{LJ}^{-1}). In our simulations, the mass of all beads was set to unity. The velocity-Verlet algorithm with a time step

of 0.005 τ_{LJ} was used to integrate equations of motion, where $\tau_{LJ} = \sigma(m/k_BT)^{1/2}$ with $k_BT=1.0$ in energy units.

The catalytic sites from which brush chains were grown were attached to the junction points of the network by the FENE bonds.
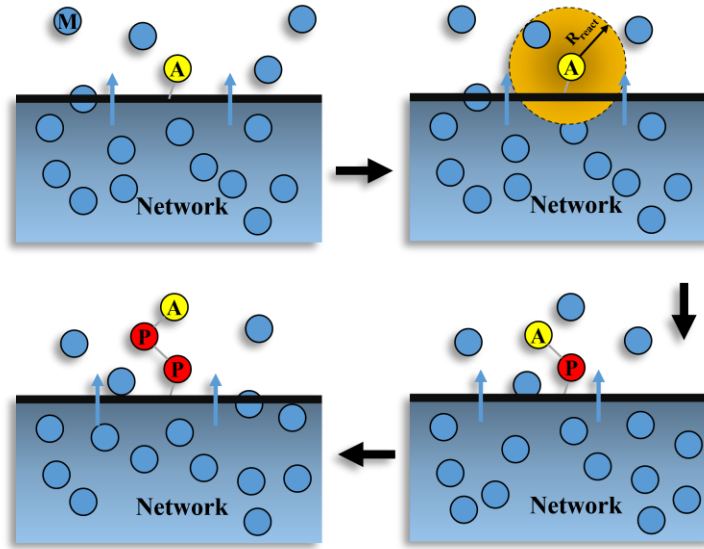

Figure S1.2: Schematic representation of main steps of monomer addition to growing brush chains.

Each simulation run was performed using the following procedure:

1) **Network swelling by monomers.** Monomers were distributed with densities $\rho=0.75\ \sigma^{-3}$ within the simulation box with the same size as a fully swollen network placed in the middle of the simulation box. Then, the system was equilibrated under NPT ($P=1.0\ k_BT/\sigma^3$) conditions until the box size reached saturation ($1.0 \times 10^5\ \tau_{LJ}$).

2) **Swollen network in a poor solvent.** After achieving network equilibration in a monomeric liquid, we changed the types of the beads located outside the swollen network to solvent. Next, the location of the network surface was determined from the density profiles of network beads and monomers. This was followed by NPT simulation run during which

remaining monomers, solvent, and network beads were redistributed within a simulation box. In particular, monomers, initially confined within a network, were squeezed out, creating a thin layer between solvent and network surface, with network strands undergoing a slight compression. This monomer layer is essential for the initial supply of monomers and selection of the direction of the brush growth.

3) **Brush polymerization.** To model the polymerization reaction and describe how fast the reaction happens, we have checked the proximity of the monomeric bead to a catalytic site every Δt_{react} = 500, 250, and 50 $\tau_{LJ,}$ which are labeled as 1x, 5x and 10x of the reaction rate (a_r). If a monomer was within a reaction cut-off radius $R_{react} = \sqrt[6]{2}\sigma$, from a catalytic site, it was added to a chain by creating a bond between the selected monomer and the catalytic site (see **Figure S1.2**).[2-3] These newly added beads became a new catalytic site (active monomer) at the end of the growing brush chains, as illustrated in **Figure S1.2**. If more than one monomer is located within the reaction cut-off radius, then only the closest one will be able to form a new bond with the catalytic site. The polymerization continued until most monomers were consumed and chain growth significantly slowed. In the current simulation setup, we limited the total number of reactions checking time N_{react} = 500.

All simulations were performed using LAMMPS[4] modified with polymerization routine.
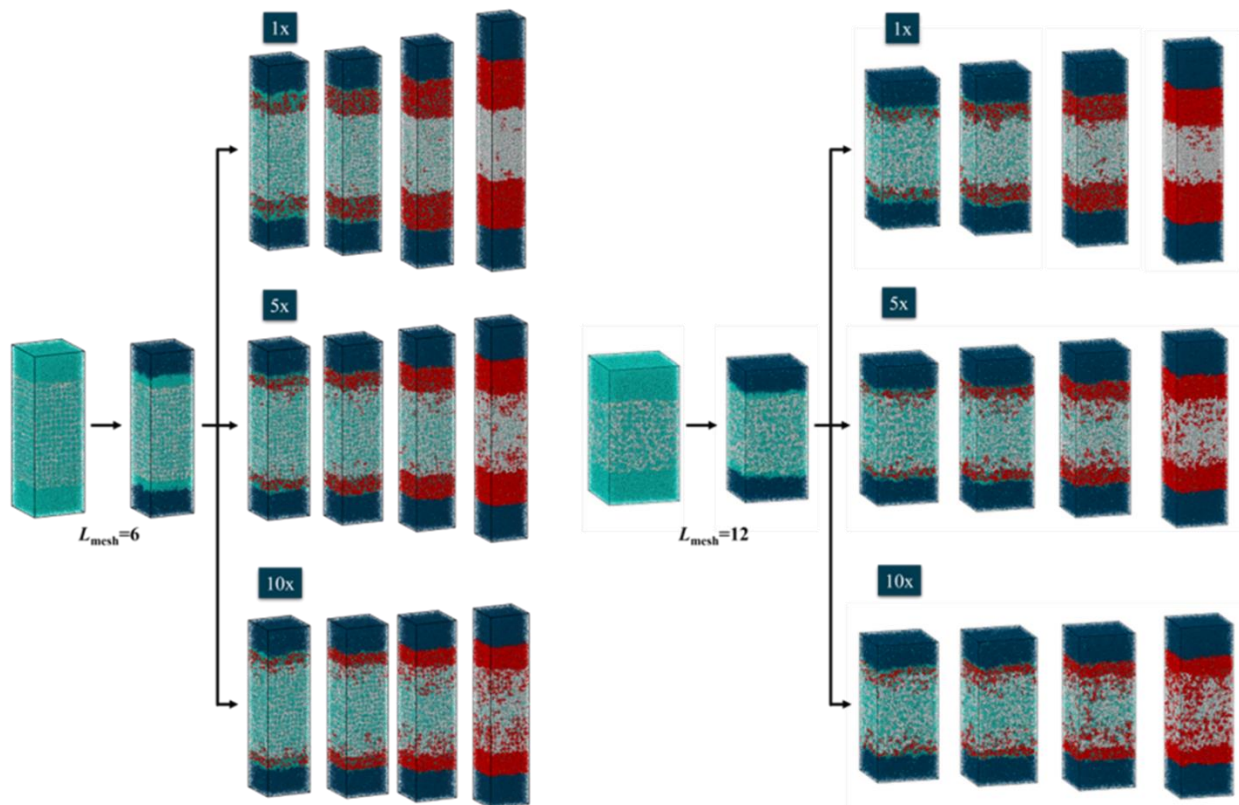
Simulation Results

Figure S2.1: Brush growth at different monomer addition rates for networks with two different mesh sizes L_{mesh}=6, and L_{mesh}=12. This figure shows that with increasing the reaction rate, brush chains end up growing inside the network. Real systems correspond to slow reaction rates below 1x and can be classified as a diffusion-controlled reaction.
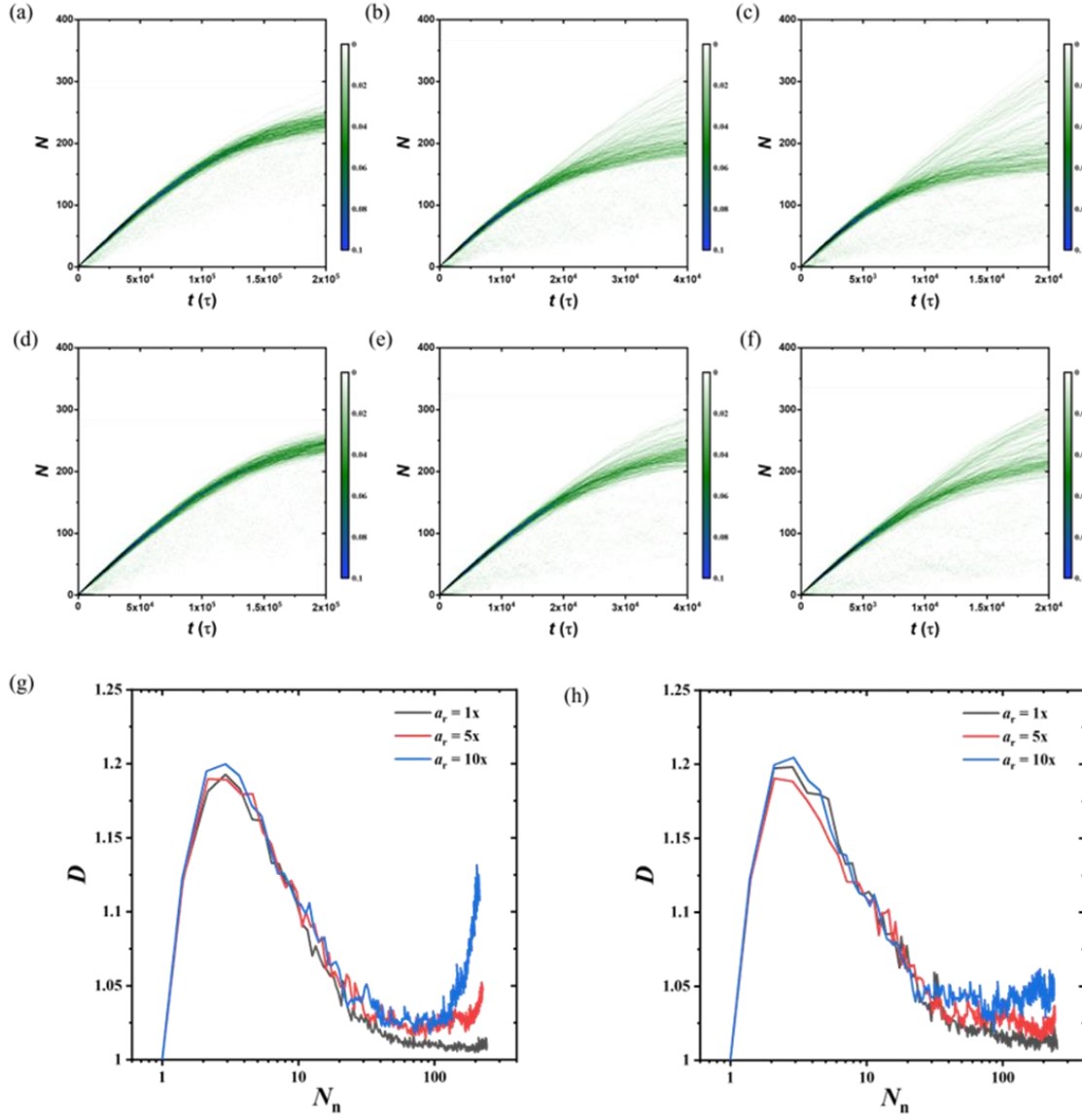
Figure S2.2: (a-f) Distribution of chains length in brush layers growing at different network mesh size and monomer addition rates (L_{mesh}=6: a:1x, b:5x, c:10x and L_{mesh}=12: d:1x, e:5x, f:10x). **(g,h)** Dispersity index of chains as a function of the number average degree of polymerization of chains in brush layers corresponding to different monomer addition rates for two different network mesh sizes (g: L_{mesh}=6, h: L_{mesh}=12).
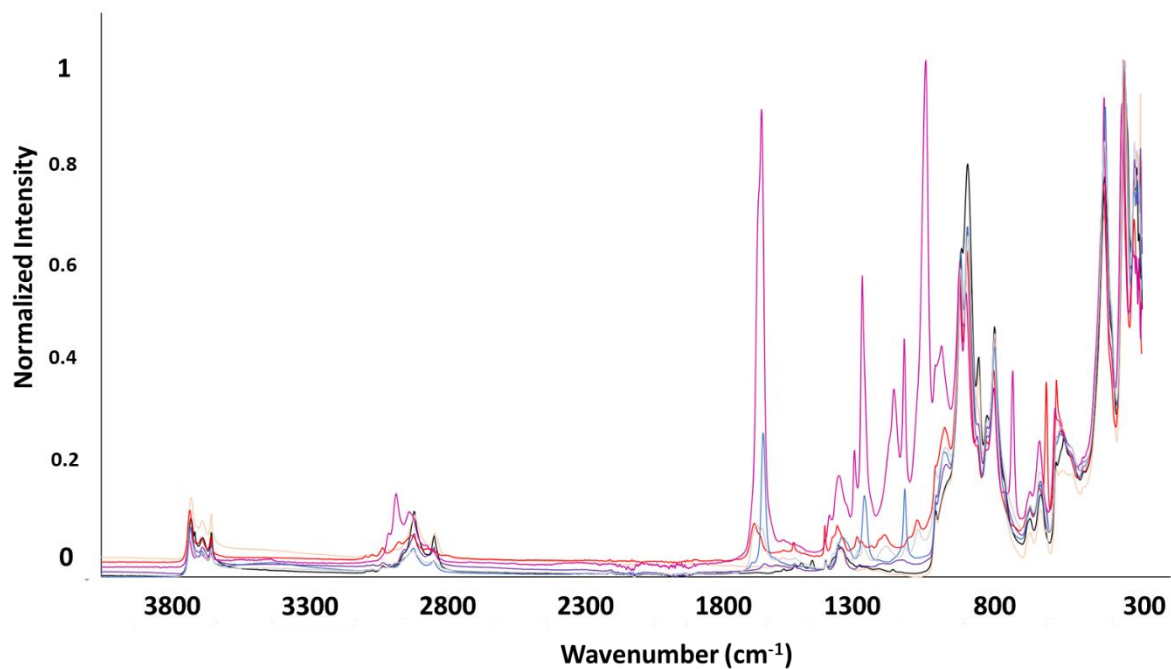
Supplemental Characterization

Figure S3: ATR spectra of all points of the functionalization process: pristine rubber (black), pretreated (orange), brominated (purple), initiator attached (red), passing-through (pink), grafting from done in water (blue), grafting-from done in acetone (gray).
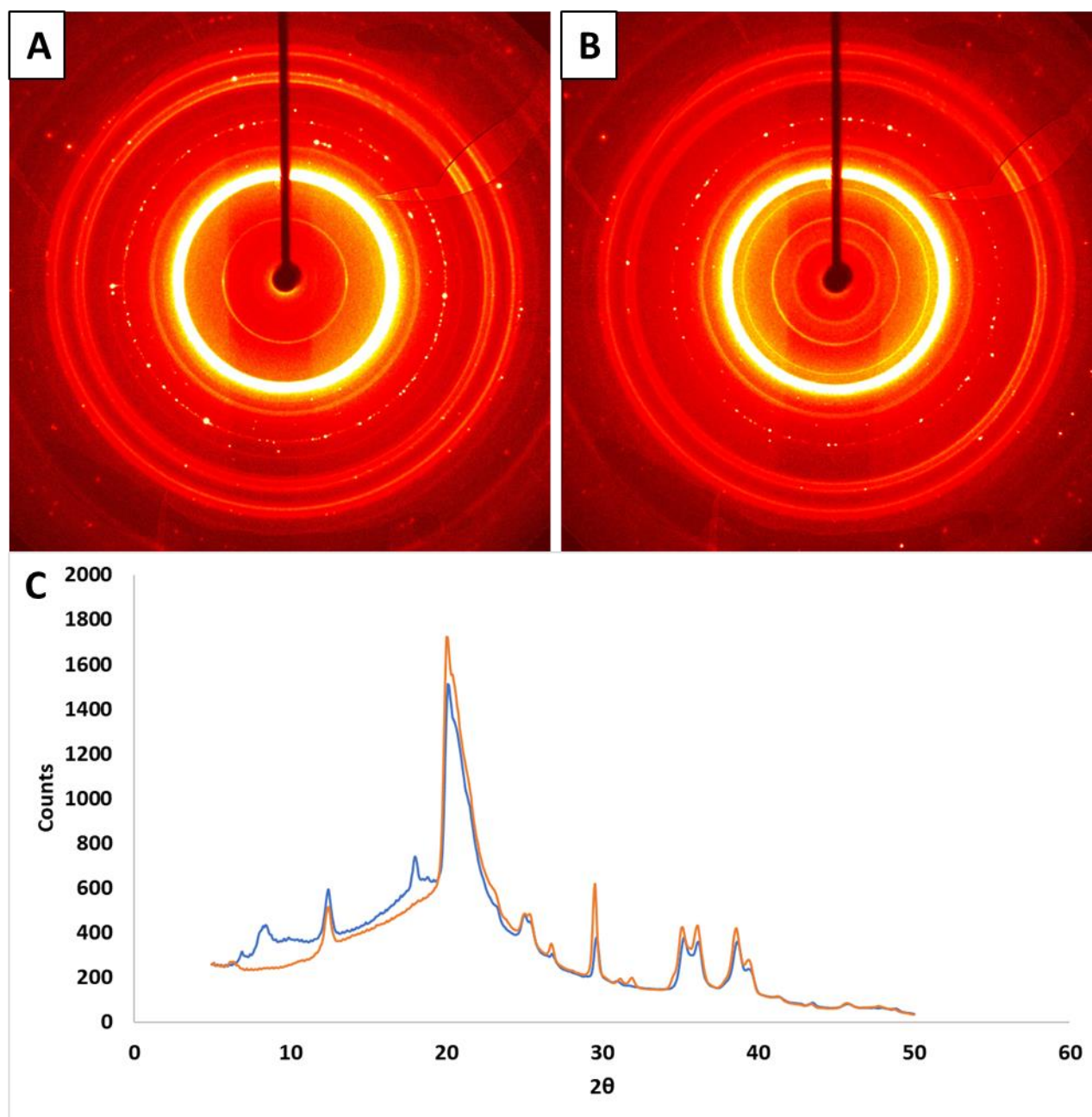
Figure S4. XRD images of the crystal structure of A) the control SBR and B) the passing through grown sample. C) Shows two spectra the blue being the passing-through sample and the orange being a control piece of SBR. The appearance of two new peaks in the blue spectra indicating the formation of new crystal structure from the polymer brushes.

For these experiments a small 1 mm thick piece of sample was cut off the top, this sample was then used for transmission mode WAXS. The sample was analyzed under a microscope to find spots of interest, once a spot was found images were taken with a spot size of 300 μm. In image B there are two more rings that appear in the image indicating a new crystal structure is present in the sample, which agrees with the FTIR. In the spectra shown in Figure S4C, there are two new peaks that appear the one ~ 17. 2 has a D spacing of 4.95, which is close to the expected spacing for crystalline P(t-BA).
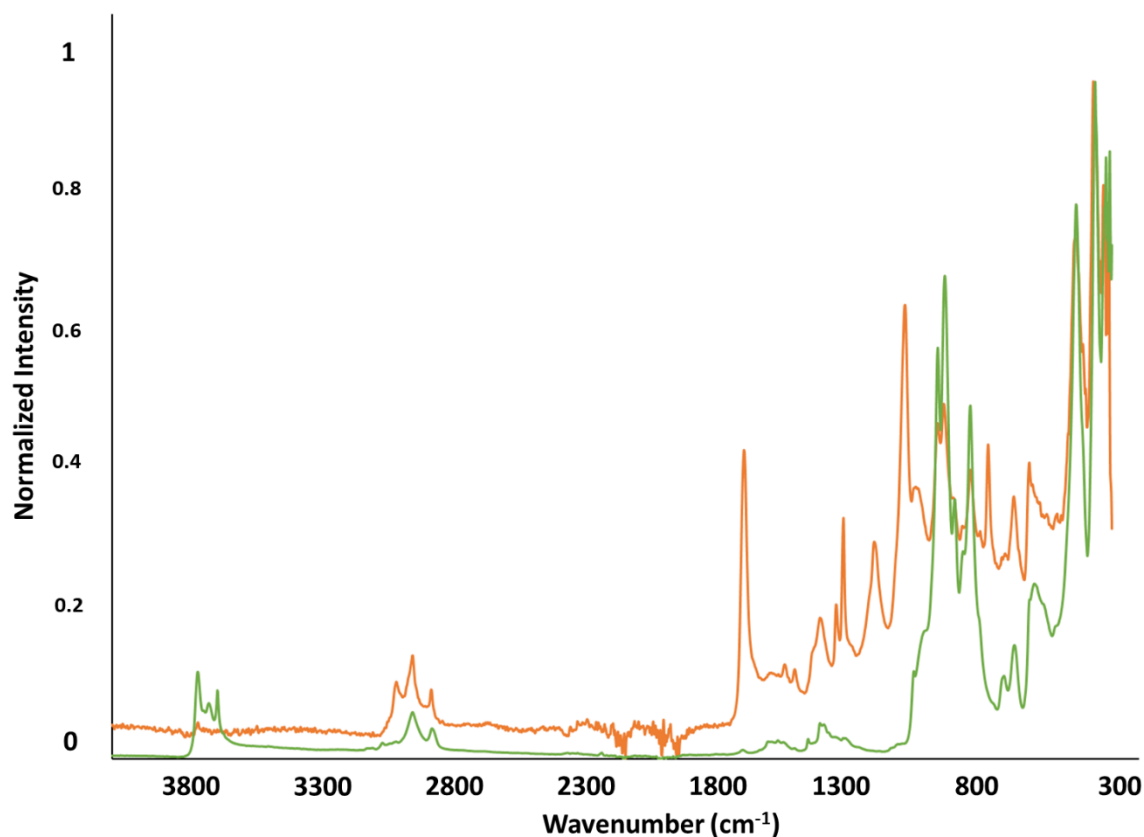

Figure S5: ATR of passing through sample where the orange spectrum is the surface of the sample and the green spectrum is the interior surface.

A sample was cut down the middle to expose the inner material allowing us to determine how deeply the polymerization takes place. Since there is a lack of carbonyls in the green spectra below, we can say not only was there little to no polymerization but there was also little to no functionalization of the interior rubber.
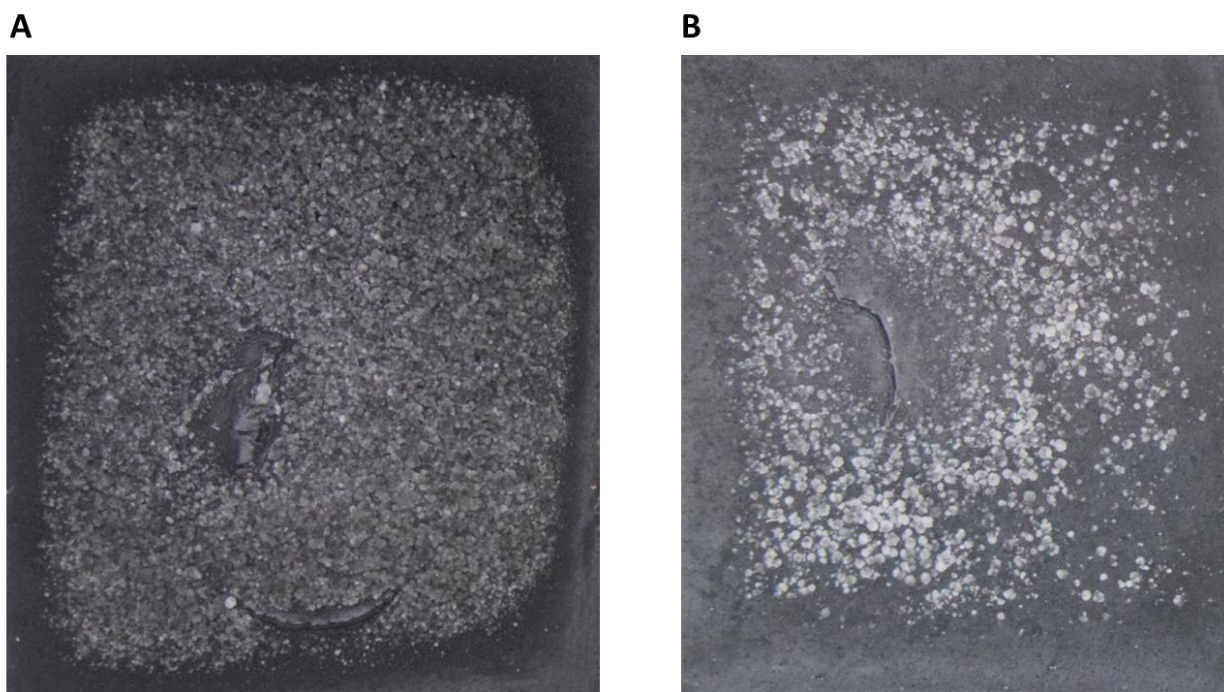
Figure S6: Images of the passing through rubbers with (A) the side facing the surface of the water. (B) the side pressed against the glass. The spherulites coverage on the right-hand side is less uniform in total coverage area as well as the size of the spherulites. We believe that the spherulites' difference here is based on the glass side sealing itself off from the solution. Preventing interaction with free copper in solution causing a higher concentration of deactivator, limiting the extent of polymerization.

S7 Bromine Content of Rubber at Different Stages of Functionalization

Sample	Wt %	Atomic %
Brominated	41.79	16.53
Initiator attached	10.09	1.92
Passing through	7.27	1.36

The weight percent of bromine has a dramatic decrease from the addition of carbon and oxygen atoms present in the initiator and the polymer backbone.
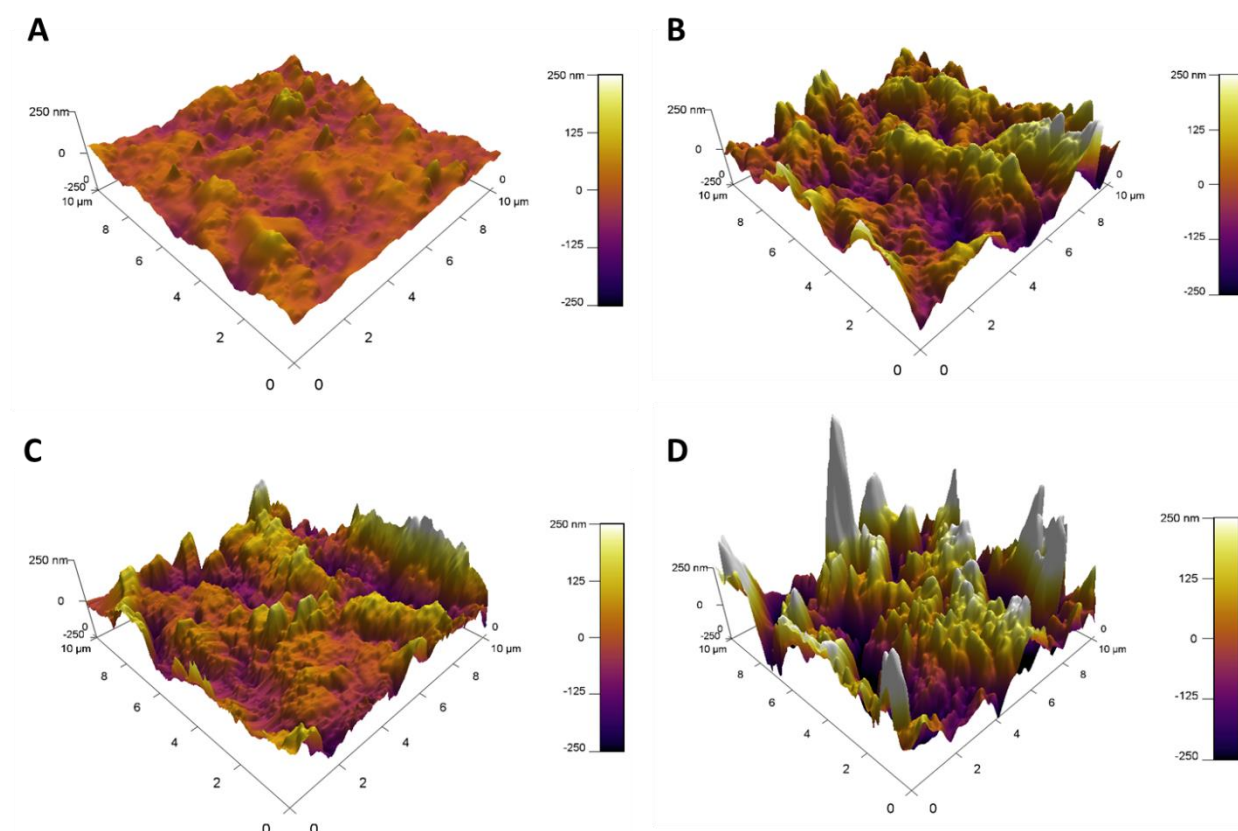

Figure S8: AFM images of the (A) pristine SBR, (B) initiator attached, (C) grafting-from, and (D) passing-through. The initiator attached sample is rougher when compared to the grafting-from sample, we believe this to be an artifact of the initiator attachment process.
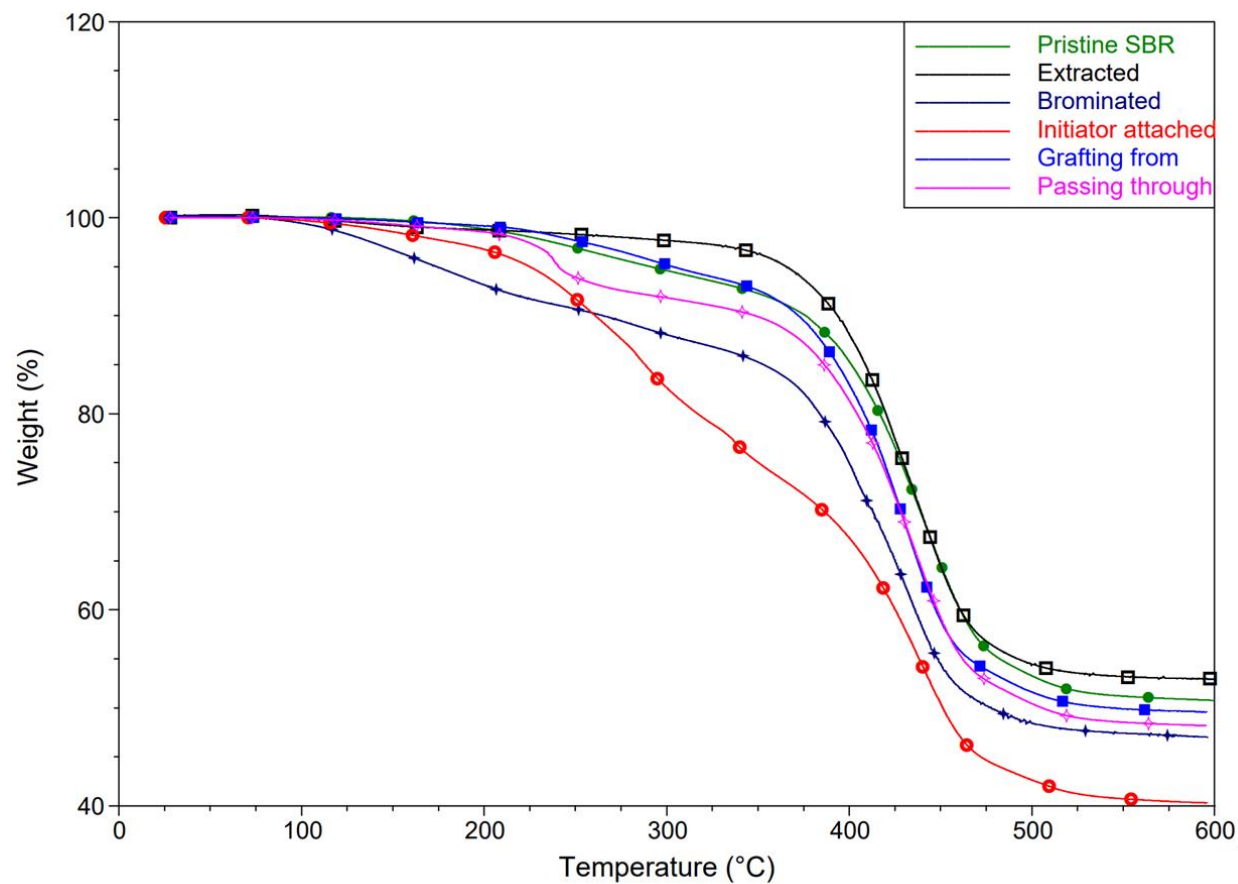
Figure S9: TGA with all steps of the functionalization. The initiator attached sample may have solvent still absorbed, leading to the large decrease in the 200 °C to 500 °C region.

References

1. Frenkel, D.; Smit, B., *Understanding Molecular Simulations*. Academic Press: New York, 2002.

2. Mohammadi Sejoubsari, R.; Martinez, A. P.; Kutes, Y.; Wang, Z.; Dobrynin, A. V.; Adamson, D. H., "Grafting-Through": Growing Polymer Brushes by Supplying Monomers through the Surface. *Macromolecules* **2016,** *49* (7), 2477-2483.

3. Wang, Z.; Liang, H.; Dobrynin, A. V., Computer Simulations of Continuous 3-D Printing. *Macromolecules* **2017,** *50* (19), 7794-7800.

4. Plimpton, S., Fast Parallel Algorithms for Short-Range Molecular Dynamics. *Journal of Computational Physics* **1995,** *117* (1), 1-19.